Crustacean Research 2024 Vol.53: 97–111

 doi: 10.18353/crustacea.53.0_97

Mysidae (Crustacea: Mysida) from sponges in sublittoral waters of Lizard Island (Indo-Pacific: Coral Sea), with description of *Heteromysis kaufersteinae* sp. nov., first record of *H. domusmaris* from nature, and range extension in *Anchialina lobata*

Karl J. Wittmann

Abstract. — The mysids *Siriella* sp., *Anchialina lobata*, *Heteromysis domusmaris* and *H. kaufersteinae* sp. nov. were extracted from sponges sampled in shallow water at the coast of Lizard Island. The range of *A. lobata* is extended ≥5400 km along waterways from the coast of SW-Australia to the Coral Sea off NE-Australia. *Heteromysis domusmaris* is first recorded from nature; this species was previously known only from coral reef aquaria. *Heteromysis kaufersteinae* sp. nov. differs from closely related species of the subgenus *Olivemysis* by the basal segment of the antennular trunk being furnished with a mid-dorsal lobe bearing a blade-like spine (modified seta), in combination with an unsegmented antennal scale, the disto-mesial edge of eyestalks bearing a tooth-like projection, by the numbers of segments of the carpopropodus of thoracic endopods 5–8, and by the numbers of spines on modified male pleopods 3–4.

LSID urn:lsid:zoobank.org:pub:22E04DFD-EA4F-4F5E-821F-A2C7FBA44835

Key words: *SW-Pacific*, *taxonomy*, *new species*, *association with sponges*, *coral reefs*

■ Introduction

During an ongoing survey of the rich material of lophogastrids and mysids in the collection of the Senckenberg Museum Frankfurt (Germany), two tubes with material extracted from sponges attracted attention by containing a total of four mysid taxa that were either new or previously unknown as being associated with sponges. Two of the below reported taxa belong to genera previously unknown from sponges. The other two taxa are species of the genus *Heteromysis* S.I. Smith, 1873. Fukuoka (2005) listed 18 species of *Heteromysis* associated with sponges. From 2004 onwards, additional species were recorded from sponges, namely *H.* (*Heteromysis*) *macropsis* Pillai, 1961, *H.* (*Olivemysis*) *cocoensis* Price, Heard & Vargas, 2018, *H.* (*O.*) *coralina* Modlin, 1987, *H.* (*O.*) *floridensis* Brattegard, 1969, *H.* (*O.*) *mayana* Brattegard, 1970, and *H.* (*O.*) *mclellandi* Price & Heard, 2011 (Price & Heard 2004, 2011, Ortiz *et al.* 2017, Price *et al.* 2018, and Daneliya 2021). The present contribution adds two other species to this list. Among the total of 108 here acknowledged (4 Feb. 2024) species of the genus *Heteromysis*, as many as 26 species — including the records presented here — have been reported as being sponge-associated, 20 of which belong to the subgenus *Olivemysis*. Little is known about the spectrum of hosts and microhabitats in mysids. The new results widen the known diversity of sponge-associated taxa and should promote future research on the function and degree of host-specificity in 'symbiotic' invertebrates.

Received: 15 Feb. 2024. Accepted: 28 May 2024. Published online: 19 Jul. 2024.

Materials and Methods

Materials

The infauna of sponges freshly sampled by SCUBA diving in shallow water at Lizard Island, Coral Sea, Australia, was washed out in the laboratory in the framework of studies on sponges and associated fauna by Silke Kauferstein (Univ. Frankfurt, Germany) in 1996. The respective formalin-fixed material was deposited in the Senckenberg Museum Frankfurt (SMF) with the label "Mysidacea" and forwarded to the present author two decades later.

Methods

The mysids were sorted in 80% ethanol and, after final examination, stored in an aqueous solution of 80% ethanol with 10% propylene glycol. Materials scheduled for mounting were treated with 4% acetic acid for 10 min and then dissected therein, finally mounted in Swan-medium (also termed 'Swann-medium') on slides. Thereafter, the slides were matured on a heat plate at 60°C for about 20 h and sealed thoroughly after several weeks. Microphotographs were produced with a Nikon DS-Fi3 Camera alternately mounted on diverse Nikon microscopes and controlled with NIS software. Some artificial coloring (in online edition) by the camera system was necessary in order to make details of the transparent objects clearly visible (Fig. 1). The length of the antennular trunk and its segments was measured along the dorsal midline. The easily confounded, large intersegmental joint between basal plate and flagellum of thoracic exopods was excluded from counts of segmental numbers.

Statolith diameters were calculated as the geometric mean of apparent length and width in ventral view. A fast and inexpensive distinction of the so far known statolith minerals was proposed by Wittmann *et al.* (1993): this orthoscopic procedure is applied using an Olympus Vanox Microscope with diascopic polarizing attachment. Cleavage and character (positive or negative) of birefringence are determined relative to a Gypsum first-order Red comparator. Fluorite (isotropic) versus vaterite plus calcite (birefringent) minerals are distinguished by their optical characteristics. Direct inspection of statolith fragment surfaces with 600x phase contrast microscopy yields cubic crystal habits in fluorite, rhombohedral habits in calcite, and elongate lense- to needle-like or nodule-shaped aggregates in vaterite (Figs. 3–5 in Wittmann *et al.* 1993). In contrast to mineral statoliths, organic statoliths shrink due to desiccation. Treatment with 0.1 N acetic acid for 1 h denaturizes organic statoliths, dissolves vaterite and calcite, but does not alter fluorite.

Terminology

Terminology as outlined *in extenso* by Wittmann & Chevaldonné (2021). Wilson (1989) defined 'whip setae' by the basal part (handle) bearing a thin flagellum (cord) separated in the present context by an articulation (Fig. 6F), suture, or at least by an optically dense section under standard microscopy. Wittmann *et al.* (2021) proposed to restrict the term 'subrostral' to frontal processes between the rostrum and ocular symphysis and to use 'epi-antennular' and 'hypo-antennular' for frontal processes (Fig. 2A) immediately above and below the antennular trunk, respectively. The hypo-antennular processes should not be confounded with a (here not treated) potential frontal process from the clypeus. Wittmann (2024) used 'distomedian lobe' for the dorsal lobe (Fig. 2B) situated behind the distal margin of the terminal segment of the antennular trunk. The terminology of gross structures of the foregut follows Kobusch (1998); modified spines of the foregut according to Wittmann & Griffiths (2018). According to the insect glossary by Moyle & Byrne (2020), 'anal lobe' indicates any protrusions near the anus; in the present context it refers to a ventral lobe of the telson bearing the anus (Fig. 6J).

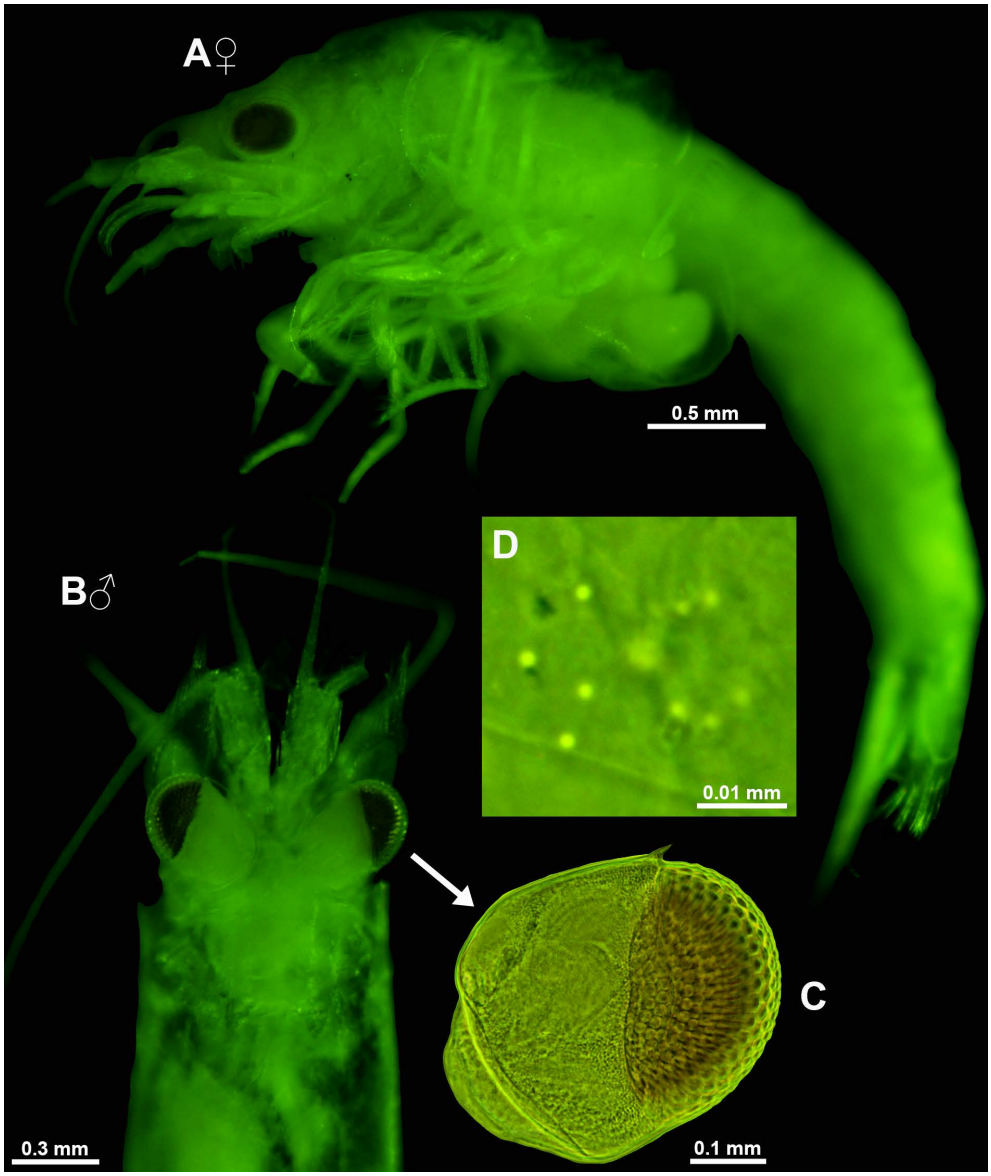

Fig. 1. *Heteromysis domusmaris* Wittmann & Abed-Navandi, 2021, adult ♀ with BL = 5.1 mm (A), and *H. kaufersteinae* sp. nov., holotype adult ♂ 4.2 mm (B–D). A, female habitus, lateral; B, anterior 2/3 of cephalothorax in male, dorsal; C, detail of (B) showing right eye; D, posterior pore group on carapace. A–C, objects artificially separated from background; objects in vial (A–B) and on slides (C–D).

Abbreviations and repository

BL = body length measured from anterior margin of carapace (tip of rostrum) to terminus of telson without spines

SMF = Senckenberg Museum Frankfurt (repository)

Taxonomic Account

Subfamily Siriellinae Czerniavsky, 1882
Tribe Siriellini Czerniavsky, 1882
Genus *Siriella* Dana, 1850
Siriella sp.

Material examined

Posterior 2/3 of 1 egged ♀, posterior half of 1 ♂ ad. (SMF-57158), Indo-Pacific, Coral Sea, Australia, Queensland, N Cooktown, Lizard Island, North Point Reef, 14°38.745′S 145° 27.255′E, 19 m depth, LI-Pr.22, SCUBA diving, sponges on rock/stone, mysids extracted *ex situ*, 20 May 1996, day, leg. S. Kauferstein.

Note

This damaged material was extracted from undetermined sponges. Residuals of tail fan and male pleopods clearly point to a species of the genus *Siriella*. The available details do not suffice for a firm determination at species level.

Subfamily Gastrosaccinae Norman, 1892
Tribe Anchialinini Wittmann, Ariani & Lagardère, 2014
Genus *Anchialina* Norman & Scott, 1906
Anchialina lobata Panampunnayil, 1999

Anchialina lobatus Panampunnayil, 1999: 685–692, Figs. 1–39 (first description, SW-Australia); Jocqué, 2002: 8, Fig. 42 (taxonomy, in key); Keable *et al.*, 2003: 432 (in list of Australian species); Wooldridge & Mees, 2015 (in worldwide database).
Anchialina lobata, Mees & Meland, 2024: AphiaID 711565 (accepted).

Material

1 egged ♀ with BL 6.1 mm, 1 ♀ subad., 1 ♂ subad., 1 juv. (SMF-57157) from same sample as given above for *Siriella* sp.

Type locality

Not defined by Panampunnayil (1999). Upon first description he reported specimens from several localities in SW-Australia, range 33°14′ S–35°16′S 114°28′E–119°29′E. Materials netted from the upper 50 m of the water column. Panampunnayil (1999) did not indicate the sampling time, which is required for checking potential diurnal migration.

Distribution

All previous records refer to the localities in SW-Australia published by Panampunnayil (1999). The present record extends the known range from SW-Australia diametrically across the continent to NE-Australia, the distance being ≥5400 km along waterways or about 3600 km air route. Currently it remains unclear whether these mysids show any specific relationship to sponges or merely use them as a chance shelter.

Subfamily Heteromysinae Norman, 1892
Tribe Heteromysini Norman, 1892
Genus *Heteromysis* S.I. Smith, 1873
Subgenus *Olivemysis* Băcescu, 1968
Heteromysis (*Olivemysis*) *domusmaris* Wittmann & Abed-Navandi, 2019
(Fig. 1A)

Heteromysis (*Olivemysis*) *domusmaris* Wittmann & Abed-Navandi, 2019: 1–15, Figs. 1–6 (first description from public aquaria); Daneliya, 2021: 41 (differences from *H. abrucei* Băcescu, 1979); Wittmann *et al.*, 2021: 518 (in citation, morphology); Wittmann & Abed-Navandi, 2021: 137 (modification of pleopods, in key); Mees & Meland, 2024: AphiaID 1379689 (accepted).
Heteromysis domusmaris, Wittmann *et al.*, 2021: 490 (in citation, aquarium population).

Material

1 egged ♀ with BL 5.1 mm, in vial (SMF-61332), from same sample as in the below described holotype of *H. kaufersteinae* sp. nov.

Descriptive notes

Adult female with BL 5.1 mm, not dissected (Fig. 1A). The three segments of antennular trunk each with a flagellate spine (plus setae), namely on mid-dorsal lobe of basal segment and on disto-mesial edge in median and terminal segments. These modified spines as in the first description (Wittmann & Abed-Navandi

2019). Basal segment of antennular trunk with a few minute barbed setae on lateral margin near basis (also found in three among six aquarium specimens). Antennal sympod with spiniform extension on outer face. Antennal scale stout, with small apical segment separated by a transverse suture. Scale reaching to half-length of terminal segment of antennular trunk. Well-developed cornea covering 1/4 of eye surface, cornea distally set on eyestalk. Eyestalks with mesial and part of anterior margin rugged by scales; anterior margin with distally set, small spiniform extension. Carapace with triangular, distally rounded rostrum. Flagellum of thoracic exopods 1–8 with 8, 9, 9, 9, 9, 9, 9, and 8 segments, respectively. Carpopropodus of thoracic endopods 1–8 with 2, 2, 2, 4, 6, 7, 7, and 6 segments. Carpopropodus 3 swollen, mesial margin with 5–6 flagellate spines in linear series (not arranged in pairs). Marsupium formed by two pairs of large oostegites (not counting rudimentary oostegite); inside five eggs with diameter of 0.35–0.38 mm. Endopod of uropods with two spines near mesial margin below statocyst; distal spine-free portion 61% length of endopod. Each lateral margin of telson with total of 17 spines, arranged in two groups separated by a bare section in between. Disto-lateral lobes each with two spines, mesial spine half as long as lateral spine. Telson cleft U-shaped with total of 16 laminae on proximal half, no laminae on distal half.

The characters available without dissection fit the diagnosis of *Heteromysis domusmaris* and also the key to the species of the subgenus *Olivemysis* given by Wittmann & Abed-Navandi (2021).

Distribution

First described by Wittmann & Abed-Navandi (2019) from the public Aqua-Terra Zoo of Vienna, where it unexpectedly appeared in coral reef aquaria. No type locality defined according to Art. 76.1.1. of the nomenclatorial code (ICZN, 1999). The here reported first record from nature, namely from the fauna associated with the sponge *Phakellia stipitata* at the coast of Lizard Island in the Indo-Pacific fits well with live coral reef materials including sponges obtained by this zoo from the Central Indo-Pacific Ecoregion (additional geographic details unavailable) via a Dutch wholesaler (DeJongMarinelife Inc., NL).

***Heteromysis* (*Olivemysis*) *kaufersteinae* sp. nov.**

LSID urn:lsid:zoobank.org:act:EA2A87F9-49F6-4644-BCA7-B85241351636

(Figs. 1B–D, 2–6)

Holotype

Adult ♂ with BL 4.2 mm, on slides (SMF-61331), Indo-Pacific, Coral Sea, Lizard Island (about 14°40′S 145°28′E), sample #4 taken upon SCUBA diving in shallow water (detailed depth unknown), extracted *ex situ* from the sponge *Phakellia stipitata* (Carter, 1881), 23 Apr. 1996, day, leg. S. Kauferstein.

Etymology

The species name is a noun with female ending in genitive singular, dedicated to Silke Kauferstein (Univ. Frankfurt, Germany), who studied sponges and associated fauna at Lizard Island, in that framework sampling four mysid species that yielded the important scientific novelties presented here.

Type locality

From the sponge *Phakellia stipitata* in shallow coastal waters of Lizard Island, Coral Sea, Indo-Pacific, about 14°40′S 145°28′E.

Diagnosis

Based on a single adult male. Rostrum (Fig. 2G) forms a triangular, distally rounded plate between the eyes, half as long as terminal segment of antennular trunk. Disto-mesial edge of eyestalks with well-developed tooth-like pro-

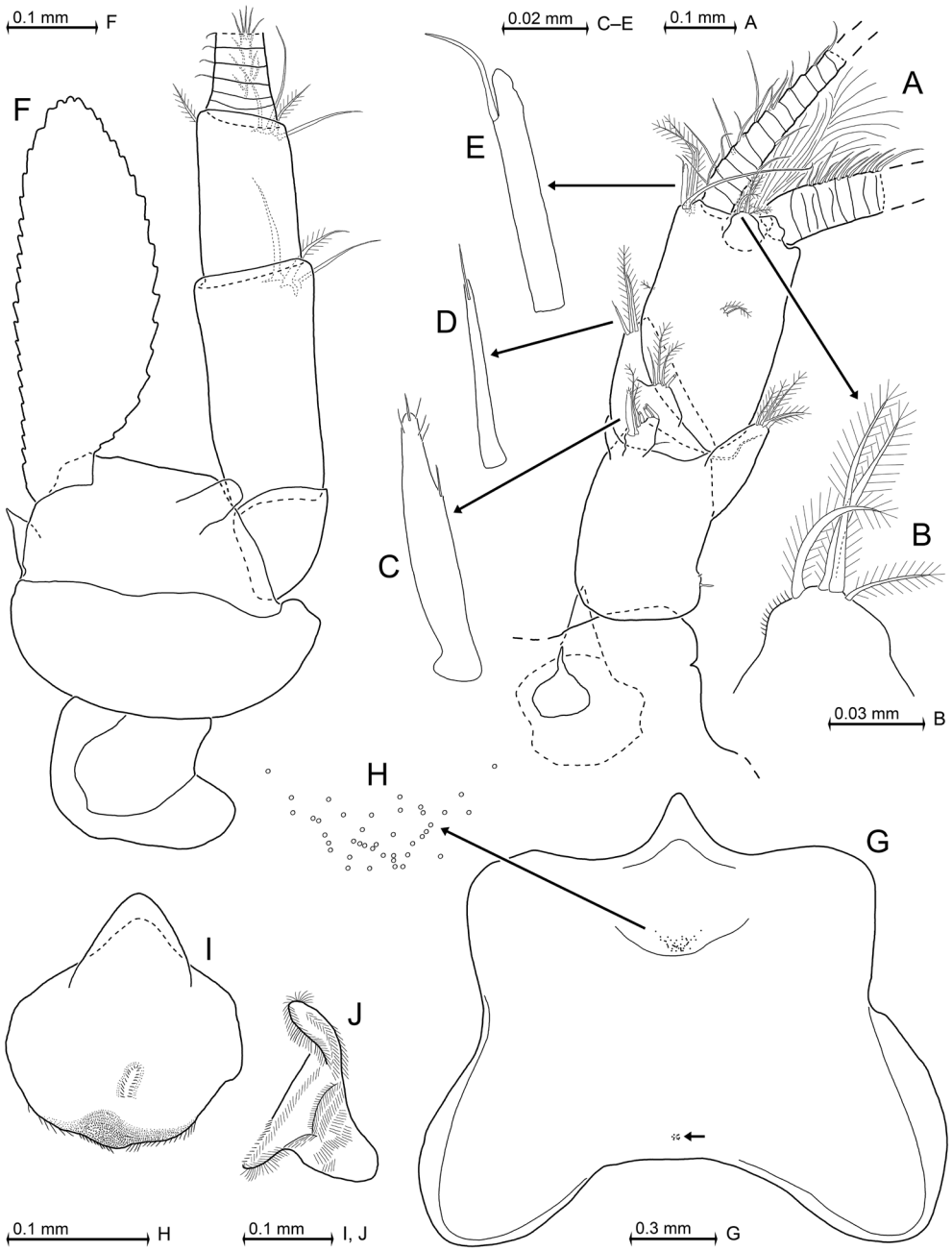

Fig. 2. *Heteromysis kaufersteinae* sp. nov., holotype adult ♂ with BL = 4.2 mm. A, antennular trunk with associated processes from the frons, dorsal; B, detail of (A) showing disto-median lobe; C–E, details of (A) showing modified spines (setae) of segments 1–3; F, antenna with antennal gland, dorsal view, setae omitted from antennal scale; G, carapace expanded on slide, small arrow points to posterior pore group; H, detail of (G) showing anterior pore group, pore diameters not to scale; I, labrum, oral face; J, left paragnath, caudal.

jection (Fig. 1C); apart from this the eyestalks with smooth surface, no scales. Well-developed calotte-shaped cornea occupies distal 25–30% of eye surface. The 3-segmented antennular trunk (Fig. 2A) with strongly oblique border between median and terminal segment, render-

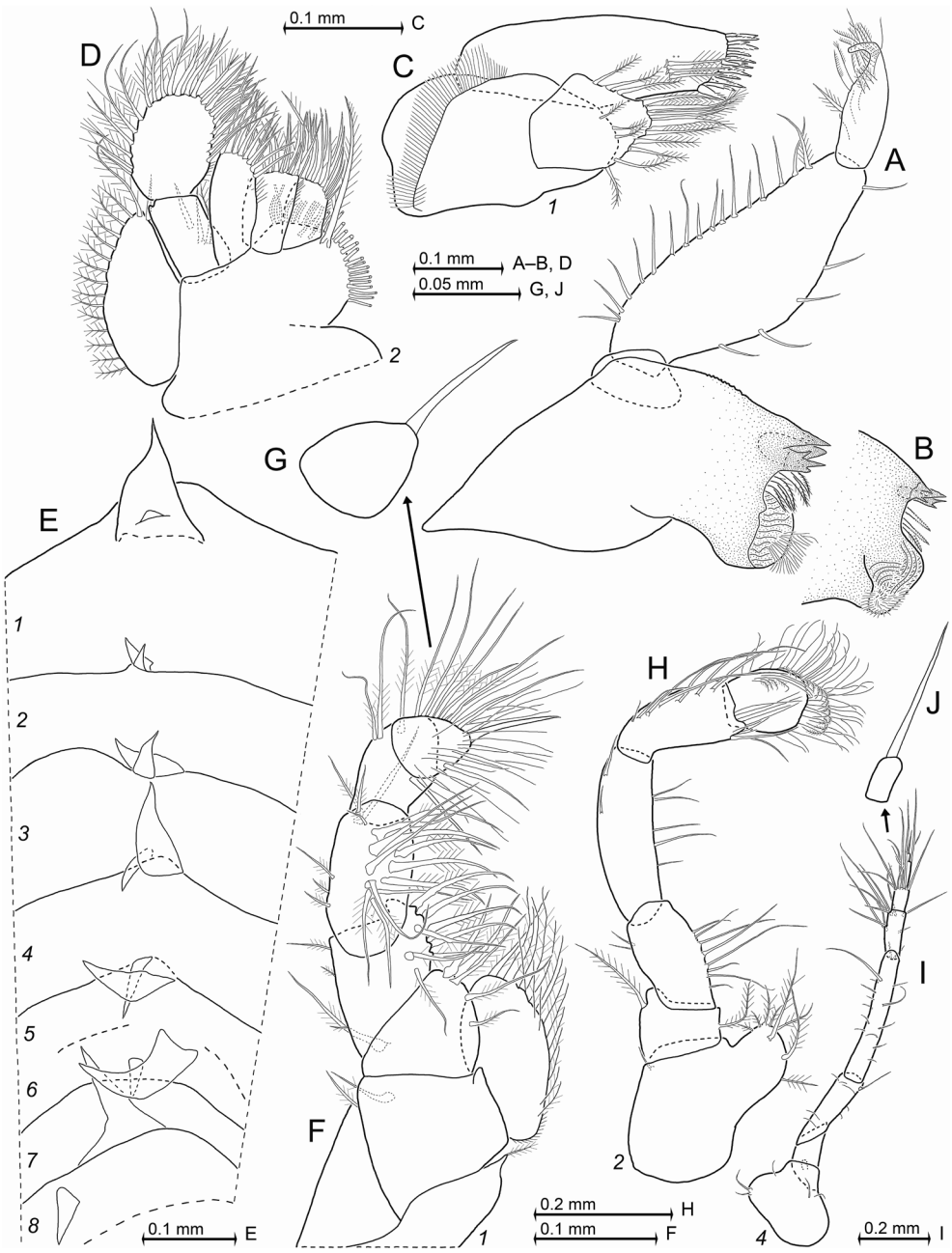

Fig. 3. *Heteromysis kaufersteinae* sp. nov., holotype adult ♂ with BL = 4.2 mm. A, left mandible with palpus, rostral; B, masticatory part of right mandible, caudal; C, maxillula, caudal; D, maxilla, caudal; E, thoracic sternites 1–8, ventral; F, thoracic endopod 1 with part of coxa, caudal; G, detail of (F) showing dactylus 1 with nail, setae omitted; H, thoracic endopod 2, rostral; I, thoracic endopod 4 with sympod, caudal; J, detail of (I) showing dactylus with nail, setae omitted.

ing the median segment wedge-shaped. Each segment with a mid-dorsal setose lobe near its distal margin; basal segment in addition with a disto-lateral lobe. Appendix masculina well developed. Trunk with three subapically flagellate spines (modified setae, Fig. 2C–E) in addition

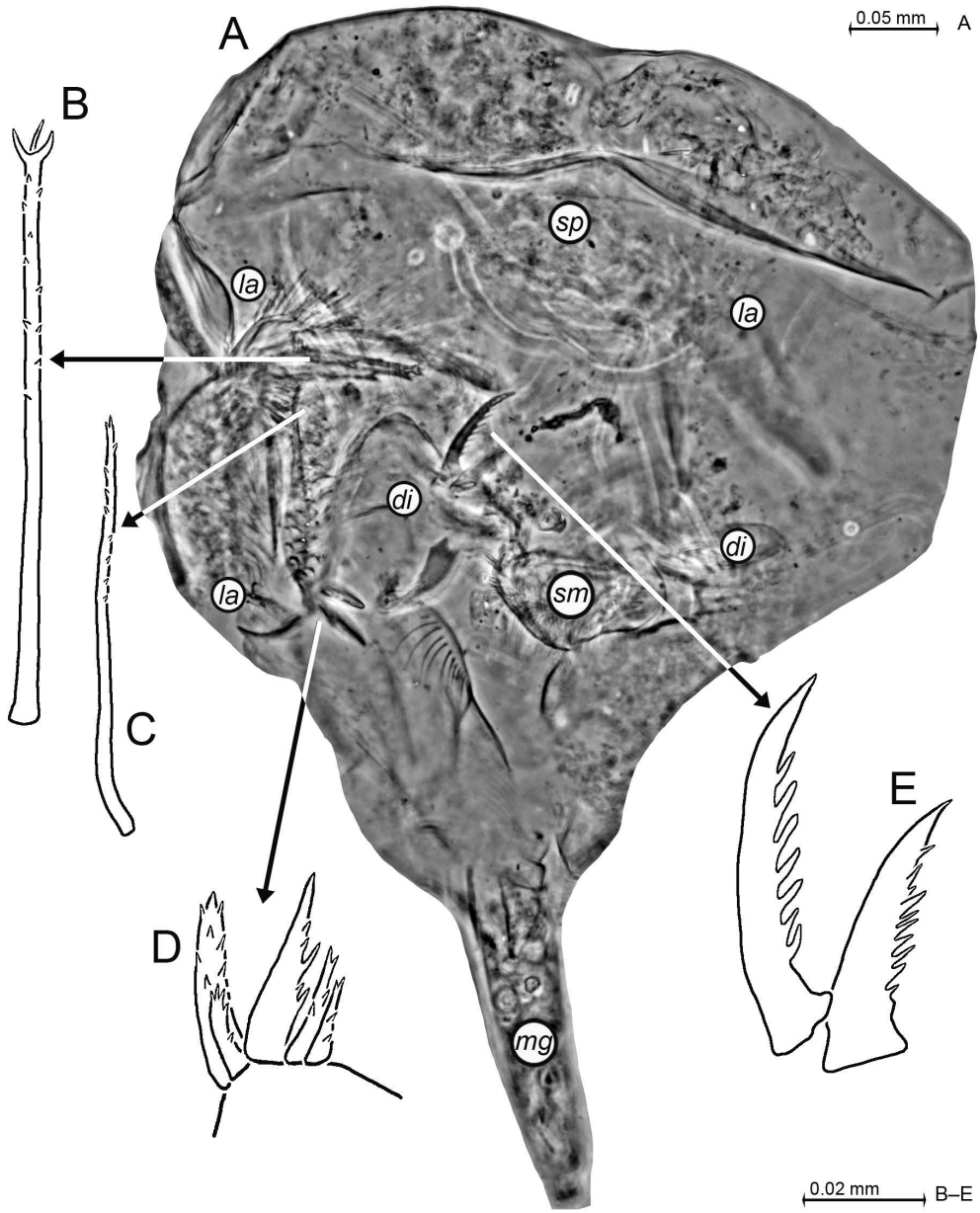

Fig. 4. Foregut of *Heteromysis kaufersteinae* sp. nov., holotype adult ♂ with BL = 4.2 mm. A, foregut with part of midgut, dorsal; B–E, details of (A) showing diverse modified spines. Lowercase labels indicate dorsolateral infolding (*di*), lateralia (*la*), midgut (*mg*), superomedianum (*sm*) and storage space (*sp*).

to normal setae, namely one spine (with short subapical flagellum and with bristles on distal half) on the mid-dorsal lobe (apophysis) of the basal segment, a shorter spine on disto-mesial edge of the median segment and a large one on disto-mesial edge of the terminal segment. Antennal scale (Fig. 2F) unsegmented, reaching to distal third of the terminal segment of the antennular trunk; its apex distanced from the distal margin of the antennal peduncle by − 1/10

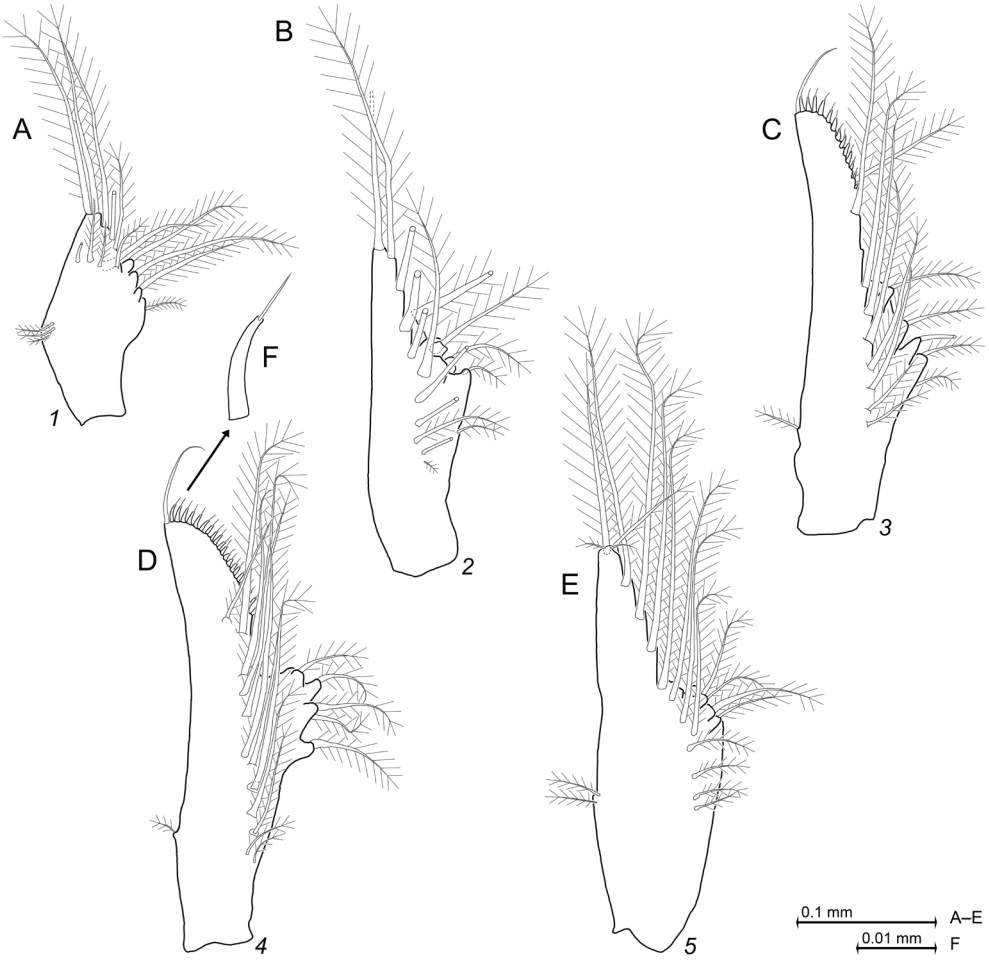

Fig. 5. Male pleopods in *Heteromysis kaufersteinae* sp. nov., holotype adult ♂ with BL = 4.2 mm. A–E, series of right pleopods 1–5, lateral = rostral face; F, detail of (D) showing flagellate spine of pleopod 4.

up to + 1/5 scale length. Scale length is 2.6–2.7 times maximum width. Labrum (Fig. 2I) with distally rounded, roughly triangular rostral protrusion. Male thoracic sternites 2–8 each with 1–2 mid-ventral, smooth triangular processes (Fig. 3E). Flagellum of thoracic exopods 1–8 with 8, 9, 9, 9, 9, 9, 9, and 8 segments, respectively. Carpopropodus of thoracic endopods 1–8 with 2, 2, 2, 3–4, 6, 6, 6, and 6 segments. Disto-mesial edge of merus 3 (Fig. 6A) without tooth-like extension. Length of carpopropodus 3 is 2.1–2.7 times maximum width; carpus and propodus separated by a distinct suture (Fig. 6B). Carpus with six flagellate spines on distal half of its mesial margin. Propodus without paradactylary setae and without spines. Penes tubular, 2/3 length of ischium of endopod 8 (Fig. 6G). Pleopods (Fig. 5) rudimentary, unsegmented, setose, with (in part indistinct) residual differentiation of the endopod (pseudobranchial lobe). Pleopods 1–2, 5 normal, no spines (Fig. 5A–B, E). Pleopods 3–4 with distal third to half knife-shaped (Fig. 5C–D), 'blade' 1/4 pleopod length; distal margin broadly rounded with small subapically flagellate spines (Fig. 5F) densely set along blade; flagella shorter than handle; pleopod 3 with 14 spines, pleopod 4 with 21–22 spines (partly

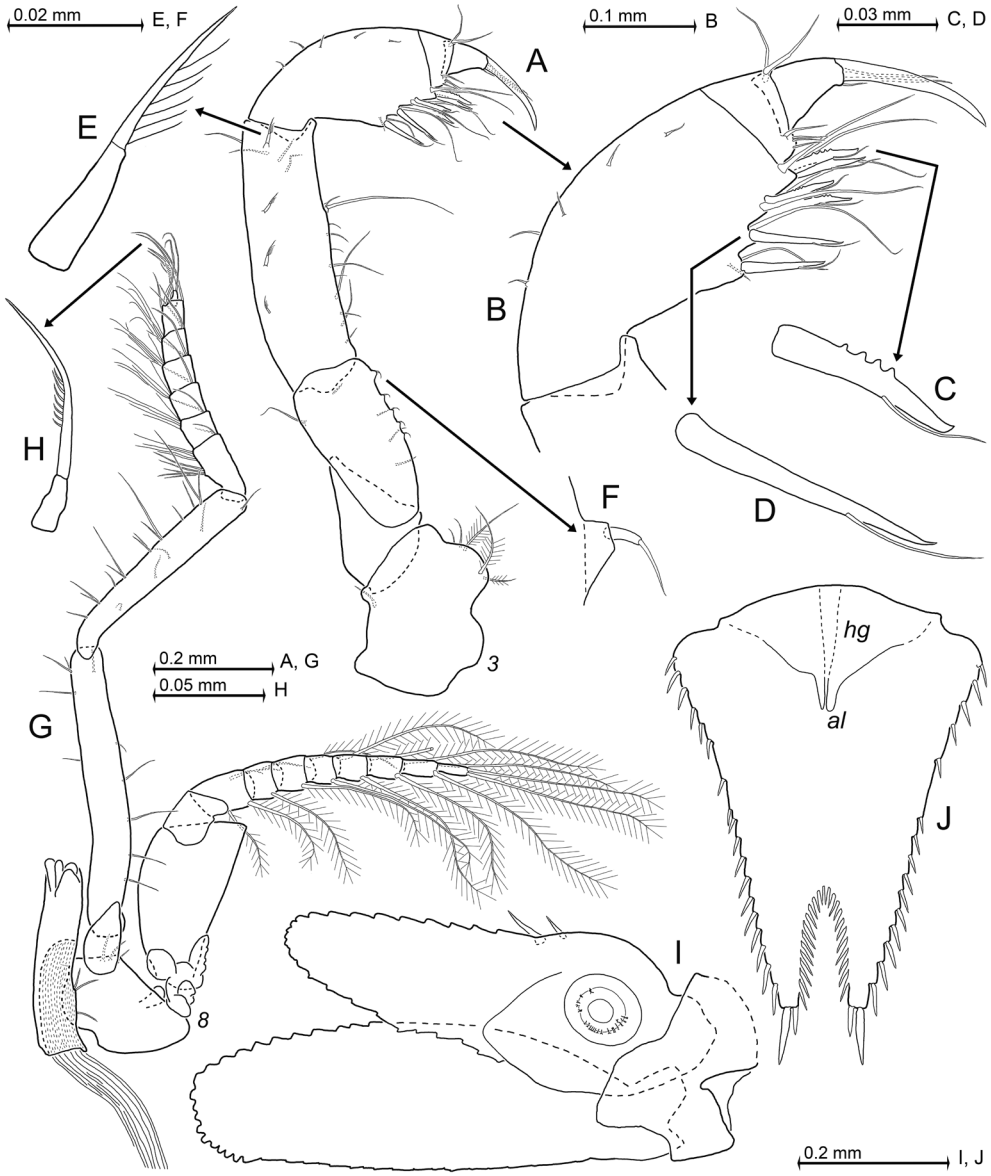

Fig. 6. *Heteromysis kaufersteinae* sp. nov., holotype adult ♂ with BL = 4.2 mm. A, left thoracic sympod and endopod 3, rostral; B, detail of (A) showing tarsus with claw; C–D, details of (B) showing second (D) and sixth (C) flagellate spine counted from basis; E–F, details of (A) showing modified setae on merus (E) and ischium (F); G, left thoracopod 8 with penis, caudal; H, detail of (G) showing dactylus with claw, setae omitted; I, uropods, dorsal view, setae omitted; J, telson with hindgut (*hg*) and anal lobe (*al*), ventral.

covered by setae in Fig. 5C–D). Exopod of uropods 1.1–1.2 times length of endopod (Fig. 6I); exopod extends 1/7 its length beyond endopod; endopod with two spines on mesial margin near statocyst. Lateral margins of telson (Fig. 6J) all along with 15–18 spines. Telson with V-shaped narrow apical cleft penetrating 28% telson length; cleft with 23 laminae all along margin. Terminal lobes of telson each with two spines, among which the disto-lateral spine is 13% telson length, the disto-mesial spine 0.4–0.5 times length of disto-lateral spine.

Description of male holotype

All features of the diagnosis. General appearance robust (Fig. 1B). Body length 4.2 mm. Cephalothorax comprises 30% body length, pleon without telson 57%, telson 13%, carapace without rostrum 26%, and rostrum 5%. Pleomeres 1–5 measure 0.9, 0.9, 0.8, 0.8, and 0.9 times the length of pleomere 6, respectively.

Carapace (Fig. 2G–H): rostrum reaches to half-length of eyestalks in normal orientation. Antero-lateral edges of carapace rounded, not projecting rostrally. Posterior margin leaves the ultimate thoracomere mid-dorsally exposed. As in many species of Mysidae, two characteristic groups of pores present on midline of carapace. The anterior group (Fig. 2H) is directly in front of the cervical sulcus and comprises 40 pores with about 1 μm diameter. The posterior pore group (Fig. 1D) is shortly in front of posterior margin of carapace; this group consisting of ten pores with about 2–3 μm diameter surrounding a larger but indistinct, rounded structure. Except for the here stated structures, carapace with smooth outer surface.

Eyes (Fig. 1B–C): eyestalks and cornea dorsoventrally weakly compressed. Cornea diameter 1.1 times the length of apical segment of antennular trunk. In dorsal view, the cornea appears calotte-shaped and measures 0.7 times length of eyestalk.

Antennulae (Fig. 2A–E): the trunk extends half its length beyond the eyes (Fig. 1B). Measured along dorsal midline, the basal segment is 40% trunk length, median segment 18%, and terminal segment 42%. Basal segment on basal half of its lateral face with one small seta. Its dorsal apophysis with five setae and a blade-like, modified spine (modified seta; Fig. 2C) on distal half bearing a small subapical flagellum and several small bristles. Lateral lobe with five setae. Median segment with two plumose setae and one short, subapically flagellate spine (Fig. 2D) on disto-mesial edge. Dorsally it bears a large apophysis with four setae. Terminal segment 1.4 times longer than wide. Its disto-median lobe (Fig. 1B) with four barbed setae, with small cilia lining the disto-mesial margin; no spiniform anterior projection. Disto-mesial edge of terminal segment with one subapically flagellate, blade-like spine (Fig. 2E) accompanied by one long, smooth seta facing disto-laterally, plus two anteriorly directed plumose setae. The lateral antennular flagellum is thicker than the mesial one by a factor of 1.4 when measured near basis of flagella. Male lobe moderately setose, inserts ventrally close to terminal margin of antennular trunk, lobe broadly rounded. Epi-antennular process subovate with small, rostrally projecting, acute projection; hypo-antennular process subcircular with acute triangular rostral projection (Fig. 2A).

Antennae (Fig. 2F): sympod dorsally with terminally rounded, tongue-like process. Disto-lateral edge of sympod with tooth-like process. Sympod caudally with bulbous lobe containing end sac of antennal gland. The 3-segmented antennal peduncle with basal segment 21% peduncle length, second segment 45%, and third segment 34%. Antennal scale with slightly convex, almost straight lateral margin and with strongly convex mesial margin; scale setose all around.

Primary mouthparts (Figs. 2I–J, 3A–B): labrum (Fig. 2I) weakly cuticularized, densely covered by short, stiff bristles. Left paragnath (Fig. 2J) with moderately stiff bristles, no tooth-like bristles. Mandibular palp three-segmented (Fig. 3A). Its proximal segment without setae, 11% length of palp. Median segment 61% palp length, its length 2.5–2.6 times maximum width. Its lateral margin almost all along with 16 smooth setae, an additional basally barbed seta in distal-most position. Mesial margin with only five smooth setae distributed with large interspaces. Terminal segment 28% palp length, its tip laterally bent. Its mesial margin bare except for some setae near apex; lateral margin well setose. Pars molaris with

well-developed grinding surface on both mandibles. Left mandible (Fig. 3A) with pars incisiva bearing four teeth, digitus mobilis with two teeth, pars centralis with five spines unilaterally furnished with acute bristles. Right mandible (Fig. 3B) with pars incisiva bearing three teeth, digitus mobilis smaller than to the left, with two teeth; pars centralis with two bilaterally finely serrated spines proximally (= orally) followed by a spine with aboral margin serrated and oral margin furnished with acute bristles.

Foregut (Fig. 4): lateralia anteriorly with group of slender, apically pronged (coronate) spines (Fig. 4B) with small denticles along distal half of the shaft. Lateralia caudally with shorter, apically pronged spines (Fig. 4C), also with small denticles along distal half. Lateralia even more caudally with cluster of five discontinuously serrated spines (Fig. 4D) of varying size. Dorsolateral infoldings with pair of larger spines that are serrated (Fig. 4E) along subbasal to subapical portions of shaft.

Maxillula (Fig. 3C): distal segment terminally with 12 strong spines, most of which are microserrated along median portions of their aboral margin. This segment subterminally with three setae barbed on their distal 2/3; two pores with diameter of about 1.2 μm closely adjoining the most aboral seta. Endite of maxillula terminally with three large, distally spiny setae flanked by numerous shorter, proximally thick, barbed setae; caudal face with three tiny barbed setae.

Maxilla (Fig. 3D) with 15 barbed setae all along lateral margin of exopod, the most apical seta larger than the remaining ones. Basal segment of endopod with three basally thick, barbed setae. Terminal segment stout, only 1.3 times longer than wide and 1.1 times length of basal segment.

Thoracic sternites (Fig. 3E): sternite 1 with large, triangular anterior lobe. This lobe bears a small, rounded ventral process, probably homologous with the median processes on sternites 2–8. Sternites 2–6 with two tooth-like, triangular median processes. Sternites 7–8 each with a single, triangular process in median position. Penes distally ending in four lobes, their basal half with three setae (Fig. 6G).

Thoracopods general (Figs. 3F–J, 6G–H): basal plate (Fig. 6G) of exopods expanded, length 1.8–2.1 times maximum width. Lateral margin of plates ends in an apically narrowly rounded edge. Thoracopod 1 with large, leaf-like, smooth epipod. Basis of endopods 4–8 (Figs. 3I, 6G) with a small, lappet-like apophysis on rostral face; no such apophysis in endopods 1–3. Ischium shorter than merus in endopods 1–4 (Figs. 3F, H–I, 6A), but longer than merus in endopods 5–8 (Fig. 6G). Thoracic endopods 1–3 each with dactylus (Figs. 3G, 6B) larger than that of endopods 4–8 (Figs. 3J, 6H). Dactyli 1 (Fig. 3G) and 4 (Fig. 3J) with slender, (almost) straight, smooth nails. Claws 5–8 more strongly bent, distal half with comb-like series of minute barbs (Fig. 6H). Combined praeischium plus ischium of endopod 2 (Fig. 3H) are 0.9 times merus length, carpopropodus plus dactylus 1.1 times merus. Dactylus 2 very large, with dense brush formed by great numbers of normal setae and 15 modified setae, the latter apically bent, bearing symmetrical series of denticles (stiff barbs) on either side in subbasal to median portions. Carpopropodus of endopod 4 (Fig. 3I) densely furnished with smooth simple setae and whip setae, no other types of setae.

Gnathopods (Fig. 6A–F): thoracic endopod 3 forms a powerful subchela. Basis with distinct but much shorter endite compared to that (Fig. 3H) of endopod 2. Ischium 2.0 − 2.1 times as long as wide; merus 3.5 times as long as wide and 1.5 times length of ischium. Distal 50–65% of ischium (Fig. 6A) with five small, proximally bent whip setae on mesial margin, each whip seta on the tip of a short trapezoid projection (Fig. 6F). Ischium and merus strong, as normal in gnathopods. Series of four unilaterally barbed whip setae (Fig. 6E) on rostral face of

merus; series of normal barbs (cilia) along median to subapical portions of these setae; no modified barbs. Carpopropodus 0.8 times the length of merus and 1.2 times ischium. Length of carpus 1.9 times maximum width. Carpus with six flagellate spines of which the distal four spines are unilaterally rugged by blunt teeth (Fig. 6C), these spines arranged in two pairs; proximal two spines longer, smooth, stand-alone (Fig. 6D).

Pleopods (Fig. 5): length without setae or spines increases in series of pleopods 1, 2, 5, 3, 4. Pleopods 1–2, 5 (Fig. 5A–B, E) with plumose or barbed setae only. Pleopods 3–4 with a single smooth seta at apex (Fig. 5C–D). All other setae plumose or barbed (not counting flagellate spines). The flagellate spines of pleopods 3 and 4 with about same shape and size.

Tail fan (Figs. 6I–J): exopod of uropods (Fig. 6I) with slightly convex lateral margin and strongly convex mesial margin. Endopod with distal spine-free portion 56% endopod length. Statoliths composed of fluorite, diameter 92–97 μm (n = 2). Telson (Fig. 6J) 1.2 times length of pleonite 6; telson about as long as endopod of uropod; anal lobe prominent. Spines on lateral margins decrease in size from basis to half-length of lateral margins and then increase in size distally. Apical cleft much deeper than wide. Cleft lined all along by acute laminae that are shorter than the pair of disto-mesial spines flanking the cleft.

■ Comparison

The new species shares the following character combination with three below-discussed species of the subgenus *Olivemysis*: endopod of uropod with two spines, telson with spines all along lateral margins (rarely with short unarmed gap at half-length) and telson cleft with laminae along more than half-length of cleft.

Heteromysis (*Olivemysis*) *sexspinosa* Murano, 1988 (only female known) differs from the new species by more (7–8 versus 6) segments of the carpopropodus of thoracic endopods 5–8 and by basal segment of antennular trunk without mid-dorsal lobe (apophysis) and without blade-like modified spine. In addition, it differs by average more (18–19 versus 15–18) spines on lateral margins of telson and by fusion of dactylus and claw of thoracic endopod 3 (Murano 1988, interpreted the propodus as a dactylus).

Heteromysis (*Olivemysis*) *murrayae* Daneliya, 2021, by more (7–9 versus 6) segments of the carpopropodus of thoracic endopods 6–8 (Daneliya 2021, counts the endopods differently), by basal segment of antennular trunk without mid-dorsal lobe (apophysis) and without blade-like modified spine, by two-segmented antennal scale, by disto-mesial edge of eyestalks with a small tubercle instead of a spiniform projection, by a short, broadly rounded rostrum, by male pleopods 3–4 with fewer flagellate spines (setae), namely pleopod 3 with 11 versus 14 spines and pleopod 4 with 14 versus 21–22 spines. Some of the specimens with three spines on endopod of uropod.

Heteromysis (*Olivemysis*) *agelas* Modlin, 1987, differs by basal segment of antennular trunk without mid-dorsal lobe (apophysis) and without blade-like modified spine, by two-segmented antennal scale, by thoracic exopod 1 with 9 versus 8 segments, exopods 2–7 with 10 versus 9 segments and exopod 8 with 10 versus 8 segments, by male pleopod 3 with 4 versus 14 flagellate spines (setae), and pleopod 4 with 5 versus 21–22 flagellate spines, finally by telson cleft with 12 versus 23 laminae.

The new species differs even more strongly from the remaining species of the subgenus *Olivemysis*. This subgenus now comprises 48 species including the new one.

■ Literature cited

Daneliya, M. E., 2021. On the mysid crustacean Genus *Heteromysis* (Mysidae: Heteromysinae) of the Tasman Sea, with notes on the

tribe Heteromysini. Records of the Australian Museum, 73: 1–50.

Fukuoka, K., 2005. A new species of *Heteromysis* (Mysida, Mysidae) associated with sponges, from the Uraga Channel, central Japan, with notes on distribution and habitat within the genus *Heteromysis*. Crustaceana, 77: 1353–1373.

ICZN (International Commission on Zoological Nomenclature), 1999. International Code of Zoological Nomenclature, 4th edition. 306 pp. International Trust for Zoological Nomenclature, London.

Jocqué, M., 2002. A preliminary study to the revision of the genus *Anchialina* (Mysidacea). 39 pp. BSc Thesis. Universiteit Gent, Vakgroep Biologie, Belgium.

Keable, S. J., Fenton, G. E. & Lowry, J. K., 2003. Mysidacea. In: J.K. Lowry & H.E. Stottart (eds.), Crustacea: Malacostraca: Peracarida: Amphipoda, Cumacea, Mysidacea. Zoological Catalogue of Australia, CSIRO Publ., Melbourne, 19.2B: 419–471.

Kobusch, W., 1998. The foregut of the Mysida (Crustacea, Peracarida) and its phylogenetic relevance. Philosophical Transactions of the Royal Society. B. Biological Sciences, 353: 559–581.

Mees, J. & Meland, K. (eds.), 2024. World List of Lophogastrida, Stygiomysida and Mysida. In: World Register of Marine Species. Instant Web Publishing. (URL: https://www.marinespecies.org/aphia.php?p=taxdetails&id=1379689).

Moyle, D. & Byrne, C., 2020. Glossary. In: The Caterpillar Key. Tasmanian Museum and Art Gallery, Hobart. (URL: https://keys.lucidcentral.org/keys/v3/the-caterpillar-key/key/caterpillar_key/Media/Html/entities/glossary.htm).

Murano, M., 1988. Heteromysids (Crustacea; Mysidacea) from northern Australia with description of six new species. The Beagle, Records of the Northern Territory Museum of Arts and Sciences, 5: 27–50.

Ortiz, M., Winfield, I. & Cházaro-Olvera, S., 2017. First record of mysid shrimps (Crustacea, Peracarida, Mysida) from the National Park Coral Reef Puerto Morelos, Quintana Roo, Mexico. Novitates Caribaea, 11: 46–50.

Panampunnayil, S. U., 1999. Two new species of Mysidacea (Crustacea), *Anchialina lobatus* and *Gastrosaccus sarae*, from South West Australia. Journal of Plankton Research, 21: 685–698.

Price, W. W. & Heard, R. W., 2004. Studies on the Crustacea of the Turks and Caicos Islands, British West Indies. V. Records of mysids from Pine Cay, Fort George Cay, Water Cay, and adjacent waters. Gulf and Caribbean Research, 16: 147–159.

Price, W. W. & Heard, R. W., 2011. Two new species of *Heteromysis* (*Olivemysis*) (Mysida, Mysidae, Heteromysinae) from the tropical northwest Atlantic with diagnostics on the subgenus *Olivemysis* Băcescu, 1968. Zootaxa, 2823: 32–46.

Price, W. W. & Heard, R. W., & Vargas, R., 2018. *Heteromysis cocoensis* n. sp. (Crustacea: Mysida: Mysidae) from coastal waters of Isla del Coco, Costa Rica. Nauplius, 26: e2018012: 1–10.

Wilson, G. D. F., 1989. A systematic revision of the deep-sea subfamily Lipomerinae of the isopod crustacean family Munnopsidae. Bulletin of the Scripps Institution of Oceanography, 27: 1–138.

Wittmann, K. J., 2024. The Mysidae (Crustacea, Mysida) of the ANDEEP I–III expeditions to the Antarctic deep sea with description of twelve new species, establishment of four new genera and with world-wide keys to the species of Erythropinae and Mysidellinae. European Journal of Taxonomy, 940: 1–180.

Wittmann, K. J. & Abed-Navandi, D., 2019. A new species of *Heteromysis* (Mysida: Mysidae) from public coral reef aquaria in Vienna, Austria. Crustacean Research, 48: 81–97.

Wittmann, K. J. & Abed-Navandi, D., 2021. Four new species of *Heteromysis* (Crustacea: Mysida) from public aquaria in Hawaii, Florida, and Western to Central Europe. European Journal of Taxonomy, 735: 133 - 175, video

in suppl.
Wittmann, K. J., Abed-Navandi, D., Dubois, M. & Chevaldonné, P., 2021. Three new species of *Heteromysis* (Crustacea: Mysida) from coral reef aquaria in Florida and Central Europe. Zootaxa, 4980: 490–520.
Wittmann, K. J., & Chevaldonné, P., 2021. First report of the order Mysida (Crustacea) in Antarctic marine ice caves, with description of a new species of *Pseudomma* and investigations on the taxonomy, morphology and life habits of *Mysidetes* species. ZooKeys, 1079: 145–227, suppl. 1.
Wittmann, K. J., & Griffiths, C. L., 2018. A new species of *Mysidopsis* G. O. Sars, 1864 from the Atlantic coast of South Africa, with supplementary descriptions of two additional species and notes on colour and feeding apparatus (Mysida: Mysidae). Journal of Crustacean Biology, 38: 215–234.
Wittmann, K. J., Schlacher, T. A. & Ariani, A. P., 1993. Structure of Recent and fossil mysid statoliths (Crustacea, Mysidacea). Journal of Morphology, 215: 31–49.
Wooldridge, T. H. & Mees, J., 2015. World List of the Mysidacea. (URL: https://www.marinespecies.org/aphia.php?p=sourcedetails&id=133573).

Addresses
Department of Environmental Health, Medical University of Vienna, Kinderspitalgasse 15, 1090 Vienna, Austria

E–mail addresses
karl.wittmann@meduniwien.ac.at